A Letters Journal Exploring the Frontiers of Physics

February 2007

EPL, **77** (2007) 40003
doi: 10.1209/0295-5075/77/40003

www.epljournal.org

Persistence of a pinch in a pipe

L. Mahadevan[(a)], A. Vaziri and M. Das

Division of Engineering and Applied Sciences, Harvard University - Pierce Hall, 29 Oxford Street, Cambridge MA 02138, USA

received 1 July 2006; accepted in final form 14 December 2006
published online 9 February 2007

PACS 02.40.Yy – Geometric mechanics
PACS 46.05.+b – General theory of continuum mechanics of solids
PACS 46.70.De – Beams, plates and shells

Abstract – The response of low-dimensional solid objects combines geometry and physics in unusual ways, exemplified in structures of great utility such as a thin-walled tube that is ubiquitous in nature and technology. Here we provide a consequence of this confluence of geometry and physics in tubular structures: our analysis shows that the persistence of a localized pinch in an elastic pipe whose effect decays as an oscillatory exponential with a persistence length that diverges as the thickness of the tube vanishes, which we confirm using simulations and simple experiments. The result is more a consequence of geometry than material properties, and is thus equally applicable to carbon nanotubes as it is to oil pipelines.

Introduction and scaling. – Thin sheets and membranes are ubiquitous in nature and technology over a range of length scales. Their mechanical behaviour is strongly determined by the geometrical separation of scales that allows out-of-plane bending deformations to be much softer than in-plane shearing or stretching deformations. This leads to all manner of interesting phenomena such as the wrinkling, draping and crumpling of thin sheets [1–5]. In all these situations, the primary focus has been on understanding how small scales arise from larger ones as energy and stress are quite literally focused strongly in response to imposed far field boundary conditions, and some progress has been made in understanding fine scales and singularities arising in these systems. A different set of questions that one can ask of these same thin structures is the effective geometric stiffening on scales much larger than the thickness induced purely by geometry. For example, it is well known [6] that a complete sphere is perfectly rigid with respect to isometric deformations, *i.e.* it cannot be deformed without stretching which would lead to changes in the metric. Similarly, a cylindrical sheet is much stiffer than its flat counterpart with the same dimensions and explains the relatively large effective stiffness of a carpenter's rule. Indeed the separation of geometric scales inherent in these structures gives them their large specific stiffness (stiffness per unit weight) and leads to strongly geometrical modes of deformation that involve global buckling on the one hand and localized modes on the other when subject to pressure, compression, twisting and bending. Here we focus on a peculiar global mode of deformation in cylindrical structures which are ubiquitous in nature and technology over a range of length scales, from carbon nanotubes and cytoskeletal microtubules to oil pipelines and grain silos. Our starting point is the simple observation that when a paper or plastic drinking straw of length L, radius R and thickness t ($L \gg R \gg t$) is pinched at an end it becomes elliptical locally, as shown in fig. 1 (try it yourself); however the deformation of the straw persists over a length that is much larger than the radius of the straw. This raises a natural question: what is the persistence length of a pinch?

Indeed even when a naturally flat relatively narrow elastic plate of width D and length $L(\gg D)$ (equivalently, we could consider a periodically pinched sheet such as a drape) is pinched at an end to make it slightly narrower so that the amplitude of the pinch is a, casual observations show that the persistence of the pinch is much larger than the width of the strip. To understand this persistence, we note that the dominant component of the curvature is transverse to the length of the sheet and scales as as a/D^2. Then the bending energy in the sheet [7] scales as $U_b \sim Et^3(a/D^2)^2 Dl_p$, where E is Young's modulus of the material of the plate, and l_p is the unknown persistence length of a pinch. Over the scale of this persistence length, the sheet is weakly curved in two orthogonal directions so that it must be stretched (since the Gauss curvature of a

(a) E-mail: lm@deas.harvard.edu

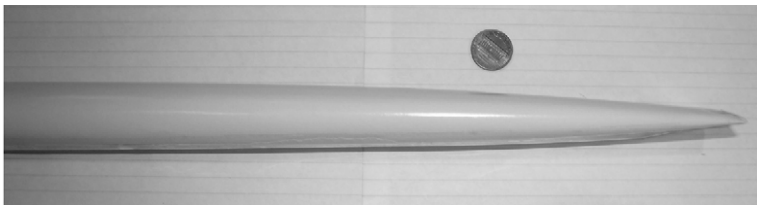

Fig. 1: A photograph of a tube pinched at an end shows that the effects of the pinch persist on scales that are much larger than the diameter of the tube. The penny in the background has a diameter of about 1 cm.

doubly curved surface is non-zero, it follows from Gauss's *theorema egregium* that it must have been stretched). The typical stretching strain associated with this deformation scales as a^2/l_p^2, costing a stretching strain energy that scales as $U_s \sim Et(a^2/l^2)^2 l_p D$. Minimizing the sum of the bending and stretching energy $U_b + U_s$, we see that the persistence length of a pinch scales as $l_p \sim D(a/t)^{1/2}$ [1,4], showing a clear dependence on the amplitude of the pinch as well as the thickness of the sheet, and diverging as the sheet thickness vanishes. When the sheet is not flat, as in the case of a complete cylindrically curved sheet of radius R, for example, a naive estimate based on the estimate just derived suggests that when such a pipe is pinched, $a \sim D \sim R$, so that $l_p \sim R^{3/2}/t^{1/2}$, a result first postulated in [8]. This somewhat surprising result suggests that the persistence of a pinch in a shell is independent of its amplitude and diverges as the thickness becomes vanishingly small. Using a combination of analysis, numerical simulations and experiment, we show that there is a unified approach to these persistent deformations in thin curved shells with possible implications for a range of systems in the microscopic and mesoscopic world.

Formulation, analysis, simulation and experiment. – To go beyond the simple scaling argument above, we start with the equations of equilibrium for a shallow cylindrical shell parametrized by its azimuthal coordinate y and the axial coordinate x, for which the von Karman-Donnell equations [9] read

$$\begin{aligned} B\Delta^2 w + \frac{1}{R}\phi_{,xx} &= w_{,xx}\phi_{,yy} + w_{,yy}\phi_{,xx} - 2w_{,xy}\phi_{,xy}, \\ \Delta^2 \phi - \frac{Et}{R} w_{,xx} &= Et(w_{,xy}{}^2 - w_{,xx}w_{,yy}). \end{aligned} \tag{1}$$

Here $A_{,b} = \frac{\partial A}{\partial b}$, $w(x,y)$ is the deflection of a point on the cylinder relative to its naturally curved state, $\phi(x,y)$ is the Airy stress function whose derivatives are the components of the in-plane stress tensor, and $B = Et^3/12(1-\sigma^2)$ is the bending stiffness of the sheet of material with Young's modulus E and Poisson's ratio σ. The first equation quantifies the balance of forces perpendicular to the cylinder surface, while the second is a geometric compatibility relation involving the in-plane strains. We note that the Karman-Donnell system is one of the simplest of a class of approximate equations of increasing sophistication for the deformations of elastic shells [10]; they assume that the curvature of the shell is small (in dimensionless terms, $t/R \ll 1$, $R/L \ll 1$) and that shear deformations may be neglected. However they are sufficient to qualitatively and quantitatively explain the phenomena at hand, as we shall see.

To mimic the effect of pinching a cylinder at one end, we assume a simple form for the prescribed displacement at the free end consistent with the first elliptical mode of deformation in the azimuthal direction. While this is undoubtedly a simplification of the localized force profile associated with a pinch, our numerical simulations of a variety of boundary conditions show that the details of how the cylinder is pinched do not affect the generic phenomena of pinch persistence that is the focus here; indeed in fig. 2 we show that an elliptical approximation to the shape is a very good one even if the shell is indented at its antipodal points. We assume that the axial variations induced are on length scales large compared to the radius, and will later check this assumption for consistency. This suggests a solution of the form $w(x,y) = W(x)\cos(\pi y/2R)$; $\phi(x,y) = \Phi(x)\cos(\pi y/2R)$. Substituting into eq. (1), and keeping only the leading order terms, we find that

$$\begin{aligned} \left(\frac{\pi}{2R}\right)^4 BW + \frac{1}{R}\Phi'' &\approx 0, \\ \left(\frac{\pi}{2R}\right)^4 \Phi - \frac{Et}{R} W'' &\approx 0, \end{aligned} \tag{2}$$

where $(.)' = \mathrm{d}(.)/\mathrm{d}x$, and we have dropped the nonlinear terms in (1). Eliminating the function $\Phi(x)$ from the above equations, we find that the amplitude of the deformation $W(x)$ satisfies the linear equation

$$W'''' + \frac{t^2}{12(1-\sigma^2)}\frac{\pi^8}{2^8 R^6} W \approx 0. \tag{3}$$

Since fourth-order equations often arise in the theory of elastic plates and shells, as a point of comparison, it is useful to recall that the balance of forces for an elastic beam supported on an elastic foundation of stiffness K yields an equation of the form [7] $BW'''' + KW = 0$. Indeed, for the axisymmetric deformations of a cylindrical shell for which $K = Et/R^2$ we also get an equation of this form, viz. $[t^2/(12(1-\sigma^2))]W'''' + W/R^2 = 0$, similar to that for a beam on an elastic foundation. While these equations might seem to be similar to (3) they

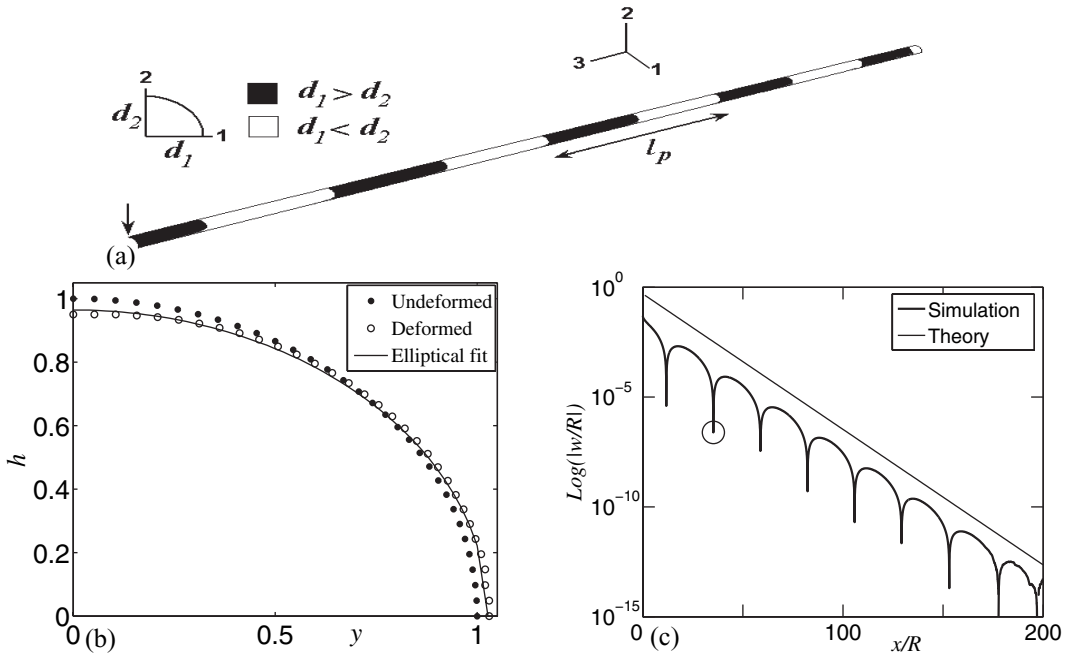

Fig. 2: Numerical simulations of pinching a cylindrical pipe ($t/R = 0.01$). (a) The ellipticity of the pipe is oscillatory. The black regions have the same ellipticity as the pinch at one end with $d_1 > d_2$, and white regions have an ellipticity that is rotated by 90° so that $d_1 < d_2$. (b) The originally circular pipe deforms into an elliptical mode in response to an indentation at its antipodal points; only quarter of the pipe is shown in light of the symmetry of deformation. (c) A log-linear plot of the scaled radial displacement of the pipe along a line parallel to the cylinder axis w/R as function of the scaled axial distance x/R from the pinch point shows that it decays exponentially. The solid line is the theoretical prediction $|w| \sim W \sim \exp(-kx)$, with k given in (4). The periodic cuspidal dips as indicated by the circle are associated with a change in sign of w when the ellipticity rotates by $\pi/2$, so that $\log|w|$ diverges, but this is of no physical significance.

are qualitatively different; in the limit of a thin shell, *i.e.* $t/R \to 0$, the preceding equation is of a singularly perturbed type exhibiting boundary-layer–like regions of size $(tR)^{1/2}$ over which the solution changes rapidly that have been the focus of many recent investigations [3]. This is quite unlike (3) which is relatively benign with no singular behavior as $t/R \to 0$. Indeed, we can see this immediately by noting that the general solution to (3) is

$$W(x) = W_0 \exp(-kx)\cos(kx+\alpha), \qquad k = \left[\frac{t^2\pi^8}{12(1-\sigma^2)2^8R^6}\right]^{1/4}, \tag{4}$$

where the amplitude W_0 and the phase α are determined by the boundary conditions at the end where the pipe is pinched. Thus an applied pinch of amplitude W_0 decays as an oscillatory exponential with a characteristic persistence length $\ell_p = 2\pi/k \sim 4.4R^{3/2}/t^{1/2}$ for typical materials with $\sigma \in [0.33, 0, 5]$. Furthermore the ellipticity induced by the pinch rotates slowly as one progresses along the pipe, analogous to the polarization of a wave. Since $\ell_p/R \sim (R/t)^{1/2} \gg 1$, our assumption that the shape and stress have variations with gradients that are much smaller in the axial direction than in the azimuthal direction is justified. Furthermore, the nonlinear terms are of order W_0/R ($\ll 1$) smaller than the linearized terms and are thus subdominant as assumed. We also observe that the persistence length is determined primarily by the geometry of the tube; the dependence on the material properties via Poisson's ratio is very weak since $\sigma \in [-1, 1/2]$ for isotropic materials. And finally we see that the persistence length of the pinch diverges as the thickness of the tube vanishes or as the radius of the cylinder diverges, *i.e.* as the tube is flattened. This geometric amplification is in sharp contrast with the focusing that leads to the generation of fine scales and singularities in the inhomogeneous deformation of thin films in such instances as wrinkling and crumpling [1–3,5].

The above-linearized analysis is valid only for small deformations in light of the approximate nature of the von-Karman-Donnell equations and our asymptotic analysis. To check the validity of our analysis, we carried out numerical simulations using the finite element method implemented in a commercial package ABAQUS that was used to minimize the elastic energy of a linear isotropic solid in a slender shell-like geometry. For very thin shells, this elastic energy density that is minimized is approximately

$$U = \frac{Et}{2(1-\sigma^2)}\left[(\epsilon_1+\epsilon_2)^2 - 2(1-\sigma)(\epsilon_1\epsilon_2-\gamma^2)\right] + \frac{Et^3}{24(1-\sigma^2)}\left[(\kappa_1+\kappa_2)^2 - 2(1-\sigma)(\kappa_1\kappa_2-\tau^2)\right]. \tag{5}$$

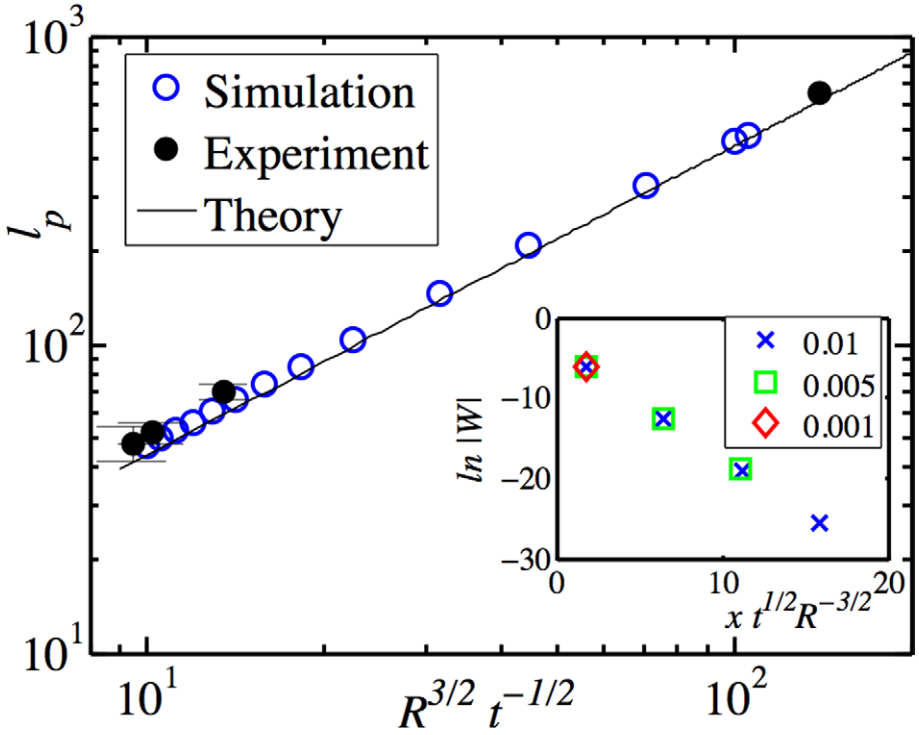

Fig. 3: Numerical simulations (circles) show that the persistence length of a pinch $\ell_p = CR^{3/2}/t^{1/2}$, with $C \approx 4.5$, consistent with experiments (triangle), and the solution of eq. (3) (solid line) to within 5%. The bars show the standard deviation of the experimental observations. Inset: we show the exponential decrease in the amplitude of the oscillatory response $W(x)$ as a function of the scaled distance $xR^{-3/2}t^{1/2}$ from the applied pinch, obtained from numerical simulations for finite deformations, in agreement with the solution of eq. (3). The symbols refers to the different values of t/R used in the simulations.

Here $\varepsilon_1, \varepsilon_2, \gamma$ are the in-plane extensional and shear strains and κ_1, κ_2, τ are the curvatures and twist relative to the undeformed state of the tube. The first term in the expression accounts for in-plane deformations and the second term accounts for out-of-plane deformations. Four-node, quadrilateral shell elements with reduced integration and a large-deformation formulation to account for the finite curvatures of the shell were used in calculations. A sensitivity study was conducted to ensure the independence of the results on the computational mesh; we refined the mesh until there was essentially no dependence of the results on the mesh size. We considered very thin isotropic and homogeneous elastic tubes which were pinched symmetrically at one end with a prescribed indentation deformation $w(0,0) = -w(0,\pi R) = W_0$; the details of the specific displacement fields that satisfy this symmetry condition turn out to be unimportant in determining the value of the persistence length of the pinch. The tubes were assumed to be made of linearly elastic material (with Young's modulus $E = 100$ MPa and Poisson's ratio $\sigma = 0.3$) of varying thickness t in our simulations, with $t \ll R \ll L$. In fig. 2a we see that the tube deforms at the location of the pinch into an elliptical shape, justifying our simple analytical ansatz. Figure 2b shows that the tube responds with a varying ellipticity consistent with our simple analytical predictions, while fig. 2c shows that the amplitude of the deformation decays exponentially as expected from our simple analysis.

In fig. 3, we show that for various t but a fixed applied pinch amplitude W_0 and tube radius R, the persistence length measured numerically by following the period of oscillation of the ellipticity also follows our analytical predictions. In the inset we show that the amplitude of the deformation of the tube decays exponentially away from the location of the pinch. We also carried out experiments with long straws and tubes of various thickness (ranging from 0.1 mm to 0.3 mm) and radii (ranging from 3 mm to 12.5 mm). The images of the pinched straws were taken with a digital camera and were analyzed using the Canny edge-detection-algorithm in MATLAB to extract the information on the boundary of the deformed profile. The thickness and radius of the tubes were measured using slide calipers. In fig. 3, we show that the experimentally measured values of the persistence length match the numerical simulations and are consistent with the scaling derived analytically over more than an order of magnitude in length. However, the oscillations are difficult if not impossible to see due to their exponential decay and their initially small amplitude at the pinch.

Discussion. – We close with a few implications of our study. On the microscopic scale, in molecular carbon

nanotubes [11,12] or cytoskeletal microtubules [8,13] our result shows how mechanical strains may be transmitted over long distances along tubes. Whether this is of any significance remains to be seen, but our calculations and experiments suggests that this persistence should be measurable; for a microtubule ($R \sim 12.5\,\mathrm{nm}$, $t \sim 2\,\mathrm{nm}$), the persistence length $\ell_p \sim 140\,\mathrm{nm}$, while for a carbon nanotube ($R \sim 2\,\mathrm{nm}$, $t \sim 0.2\,\mathrm{nm}$), $\ell_p \sim 30\,\mathrm{nm}$. Since the energy required for the deformation of a tube per wavelength scales as $Et^3(W_0/R^2)^2\ell_p R \sim W_0^2 E t^{5/2}/R^{3/2}$, this effect will persist even in the presence of thermal fluctuations as long as the elastic energy is larger than $k_B T$, *i.e.* if the amplitude of the pinch is larger than some threshold.

On mesoscales, a dramatic example of the failure of tubes is afforded by the pressure driven flip-flop propagation of buckles in submarine pipelines [14], wherein a metal pipe flattens alternately in one direction and then in an orthogonal direction, with a sharp transition region separating them. Experiments [15] show that these regions of orthogonal flattening have a characteristic length scale. Our result complements numerical simulations of the process [15] by providing a simple physical explanation for the flip-flop which we interpret as a consequence of a globally deformed tubular shell induced for example by a local perturbation. Then, an oscillatory elliptic mode follows naturally, and sets the stage for dynamic and plastic buckling that leads to a flip-flop mode of propagation. Substituting in values of the pipe diameter and thickness ($R \sim 5\,\mathrm{cm}$, $t \sim 0.5\,\mathrm{cm}$), we estimate the flip-flop wavelength to be of the order of $\ell_p \sim 4.4R^{3/2}/t^{1/2} \sim 60\,\mathrm{cm}$ which compare well with the experimentally measured values in the range of $\sim 80\,\mathrm{cm}$ [15]. The quantitative discrepancy seen is possibly due to two effects that oppose each other: a) the persistence length is reduced in a dynamic problem due to the effects of inertia, and b) the effect of a uniform pressure that acts on the tube increases the effective persistence length.

The geometric stiffening that we have studied is also used by nature in the long semi-cylindrically bent leaves that are stable against gravitationally induced buckling, and in everyday objects such as a novel paper holder that holds a sheet in a curved template for much the same purpose. Our calculations need be modified to account for natural geometries other than cylinders, *e.g.* conical and weakly elliptical shells, as well as the new scales introduced by gravity and suggest further venues of study motivated by these observations.

REFERENCES

[1] Lobkovsky A. and Witten T., *Phys. Rev. E*, **55** (1997) 1577.

[2] Ben Amar M. and Pomeau Y., *Proc. R. Soc. London, Ser. A*, **453** (1997) 729.

[3] Cerda E. and Mahadevan L., *Phys. Rev. Lett.*, **90** (2003) 074302.

[4] Cerda E., Mahadevan L. and Passini J., *Proc. Natl. Acad. Sci. (USA)*, **101** (2004) 1806.

[5] Cerda E. and Mahadevan L., *Proc. R. Soc. London, Ser. A*, **461** (2005) 671.

[6] Hilbert D. and Cohn-Vossen S., *Geometry and the Imagination* (Chelsea, New York) 1952.

[7] Landau L. D. and Lifshitz E. M., *Theory of Elasticity*, 3rd edition (Pergamon, New York) 1986.

[8] de Pablo P. J., Schaap I. A., MacKintosh F. C. and Schmidt C. F., *Phys. Rev. Lett.*, **91** (2003) 098101.

[9] Donnell L. H., *Beams, Plates and Shells* (McGraw-Hill, New York) 1975.

[10] Libai A. and Simmonds J. G., *Nonlinear Theory of Elastic Shells* (Cambridge University Press, Cambridge) 1998.

[11] Harris P. J., *Carbon Nanotubes and Related Structures – New Materials for the Twenty-first Century* (Cambridge University Press, Cambridge) 1999.

[12] Srivastava D. and Wei C., *Appl. Mech. Rev.*, **56** (2003) 215.

[13] Howard J., *Mechanics of Motor Proteins and the Cytoskeleton* (Sinaeur, Sunderland) 2001.

[14] Palmer A. C. and Martin J. H., *Nature*, **254** (1975) 46.

[15] Park T.-D. and Kyriakides S, *Int. J. Mech. Sci.*, **39** (1997) 643.